Automated planning approaches for non-invasive cardiac valve replacement procedures from CT angiography
Gao, X.; Gao X.

Citation
Gao, X. (2017, November 7). *Automated planning approaches for non-invasive cardiac valve replacement procedures from CT angiography. ASCI dissertation series*. Retrieved from https://hdl.handle.net/1887/57132

The handle http://hdl.handle.net/1887/57132 holds various files of this Leiden University dissertation

Author: Gao, Xinpei
Title: Automated planning approaches for non-invasive cardiac valve replacement procedures from CT angiography
Date: 2017-11-07

2

Automatic Extraction of Arterial Centerline from Whole-body Computed Tomography Angiographic Datasets

Xinpei Gao, Shengxian Tu, Michiel A. de Graaf, Liang Xu,
Pieter H. Kitslaar, Arthur J.H.A. Scholte, Bo Xu, Johan H.C. Reiber

Abstract

The aim of this study was to develop a new, fully automated approach for the extraction of arterial centerlines from whole-body computed tomography angiographic (CTA) data sets for the planning of transcatheter aortic valve replacement (TAVR) procedures by the transfemoral approach. The method starts with an image pre-processing step to correct contrast inhomogeneities in different image slices, followed by the detection of anatomical landmarks and subsequent wave propagation, generating a cost matrix that represents the wave traveling time. Finally, the arterial centerlines are extracted from the aortic root to the femoral arteries using the conventional Dijkstra algorithm. 36 patients who underwent TAVR procedures with whole-body CTA scans were studied; 15 for training and the remaining 21 for testing. In 1 training case and 2 testing cases, user interaction was needed to correct the centerline (in the femoral artery). In the remaining 33 cases (91.7%), a fully-automated centerline was obtained with excellent results. In all cases, the average root mean square error was 2.55 ± 0.70 mm (training 2.26 ± 0.48mm versus testing 2.77 ± 0.77 mm, $p = 0.03$) and the average mean error was 1.63 ± 0.40 mm (training 1.46 ± 0.35 mm versus testing 1.74 ± 0.39 mm, $p = 0.02$).

2.1 Introduction

Aortic valve stenosis is frequently seen in the elderly population. A severe aortic stenosis usually requires aortic valve replacement, which was the exclusive domain of open heart surgery until recent developments. The replacement is associated with a high surgical risk in elderly people, who may have various comorbidities such as porcelain aorta, pulmonary or hepatic disease, chest deformities, renal impairment, prior stroke, peripheral vascular disease, and reduced left ventricular function (Achenbach et al. 2012).

Over the past decade, Trans-catheter Aortic Valve Replacement (TAVR) has been developed as an attractive alternative for open heart surgery with likely fewer complications. One important planning step prior to TAVR is the assessment of the quality of the access pathways for the trans-catheter heart valve. This is usually done on the basis of a multi-slice computer tomography angiography (CTA) whole-body scan, including the heart and the entire femoral access route. Analytical software tools should be able to facilitate such investigations. The first step in such a tool would be to find the centerline of the entire trajectory as automatically and robustly as possible. Once an accurate centerline of the access route is available, the next step will be to calculate the cross-sections of the arteries, to determine the tortuosity, the presence and extent of calcium deposits, etc. These parameters are important indicators for assessing the risk of complications.

The goal of this study was to develop a fully automatic approach for extraction of arterial centerlines in the entire femoral access route. The approach was validated on CTA datasets that were routinely acquired prior to the TAVR procedures.

2.2 Methods

Based on our experiences, we have implemented a fully automated centerline extraction for the TAVR application. Our method extracted intensity and shape information of target arteries, and constructed a cost function representing the speed of the subsequent wave propagation. After performing the propagation implemented as a fast marching algorithm (Adalsteinsson and Sethian 1995), the Dijkstra algorithm (Dijkstra 1959) was applied to extract the centerlines of the target arteries.

Preprocessing

The CTA image was first resampled to reduce computer processing time. Next, a sigmoid filter was used to attenuate the intensity of tissues besides contrast arteries and bones. The bones near the femoral artery were removed automatically by steps including thresholding, closing, and connect component analysis. The result image was subsequently transformed into a binary image, representing the possible vascular objects. A distance transform function was constructed by applying the 3D Euclidean Distance Transform to the binary image.
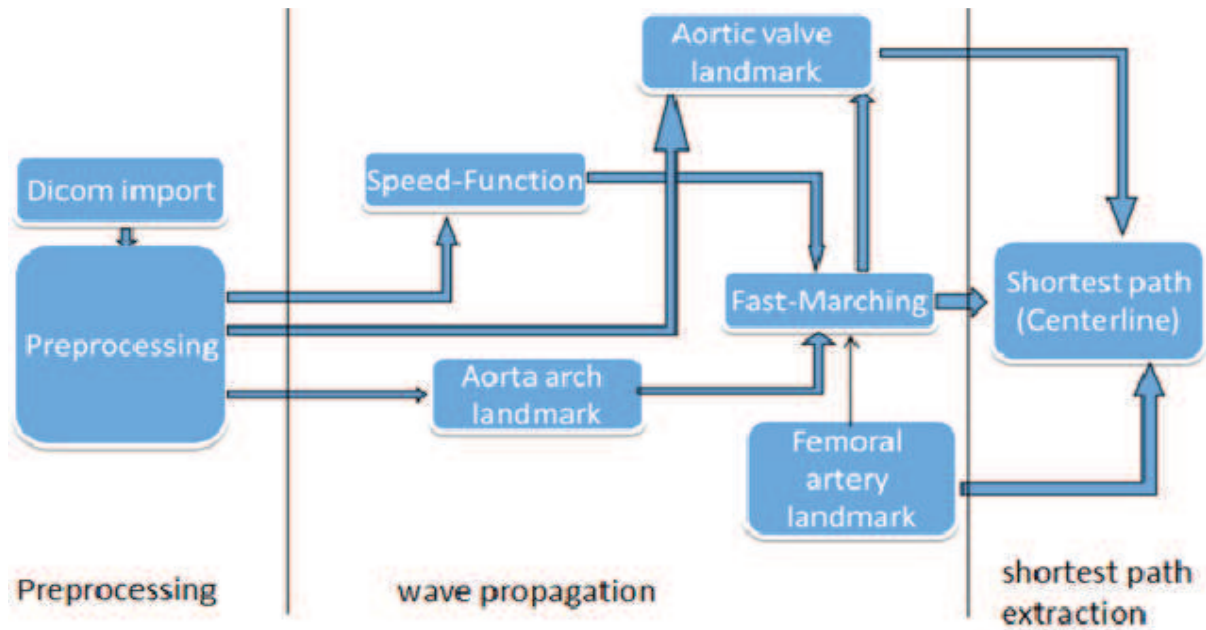
Figure 2.1. Scheme of automatic centerline extraction.

Wave propagation
Aorta arch landmark
The wave propagation requires a start point to initialize the propagation. We chose the aortic arch as the start position. Prior knowledge about the aorta diameter from literature (Mao et al. 2008) was included in the following Gaussian distribution model S(x) (Metz et al. 2009).

$$S(x) = \exp(-\frac{(D(x) - \mu_s)^2}{2\sigma_s^2})$$

Where μ_s was set to the radius of the aorta and σ_s controls the range of radii. The resulting value of S(x) is a measurement of the probability of the value D(x) belonging to the range of aorta diameters. With Distance Transformation result and this Gaussian Model, we can achieve the probability map. The aortic arch will be the biggest cluster constructed by high probability voxels at the top of CTA image.

Wave propagation
The cost function of the wave propagation algorithm was calculated based on a voxel's 3D Euclidean Distance value and its intensity value. The cost for the wave to travel inside the artery was lower towards the centerlines of the arteries. In our implementation, the wave initiated at the landmark inside the aortic arch, propagated into the ascending aorta, the aortic root on one side, and into the descending aorta, the abdominal aorta, the iliac arteries and the femoral arteries on the other side. A direction of 8-connectivty was applied in the wave propagation.

The wave stopped when it reached the aortic root on one side and the femoral arteries on the other side. These two landmarks were automatically detected by the following criterions:

First criterion was the femoral artery landmark: In our application, the wave propagated until it reached both the left half and the right half of the bottom slices in the CTA image. And the first point to reach in the left half bottom slice was the end point of left femoral artery, and the first point in the right half was the end point of right femoral artery.

Second criterion was the aortic root landmark: From the aortic arch landmark, the wave propagated to the other side through the ascending aorta and to the aortic root. The point that propagated the fastest in the left side of the slice is the center of the aorta. When the wave front propagated into the aortic valve, the wave front would split into 2 parts or 3 parts because the aorta valve has 2 cusps or 3 cusps. The 3D Euclidean distance value of the fastest point in aortic valve will be equal to or smaller than ½ of the average value of the distance of former fastest points in descending aorta.

Path extraction

After the wave propagation, each voxel was assigned a value representing the cumulative time for the wave to travel from the start point to this voxel. Inside the arteries, the wave travelled fast and the associated arrival time was shorter when compared to the voxels outside the arteries.

The Dijkstra algorithm was executed twice to get the centerlines from aortic root landmark to the left and right femoral arteries, separately. From these two centerlines, the aortic bifurcation was found and the entire access path, including the aorta segment, the left femoral segment and the right femoral segment, of the TAVR procedure using the femoral artery as the site of puncture was extracted.

2.3 Validation

Study population

This study was validated on a total of 36 patient's CTA datasets that were routinely acquired prior to the TAVR procedures. 15 datasets were randomly selected and used for training of the algorithm: 11 from Leiden University Medical Center (LUMC), Leiden, the Netherlands and 4 from Fu Wai Hospital, Beijing, China. The remaining 21 datasets were used for testing: 9 from LUMC and 12 from Fu Wai Hospital.

CTA acquisition protocol

The CTA datasets from LUMC were acquired on a 320-row volumetric scanner (Aquilion ONE, Toshiba Medical System, Japan) using Helical scan protocol. A bi-phasic injection of intravenous contrast was used: 70ml contrast (5ml/sec) and 50ml saline (5ml/sec) (de Graaf, Schuijf, van Velzen, Kroft, et al. 2010). The datasets from Fuwai Hospital were acquired by SOMATOM Definition Flash (Siemens, Germany) using Helical scan protocol. A single-phasic injection of contrast was used 350mgI/ml (3-4ml/s).The image resolution of the CTA image was 512 × 512. Approximately 1000 image slices were obtained per case.

Measurement of extraction error

An analyst delineated the corresponding centerlines semi-automatically in all cases and the results were reviewed by another analyst. Correction

was applied when there was disagreement until consensus was reached. The delineated centerlines were used as the reference standard; the extraction error was defined as the distance between the reference centerline point and the closest point in the automatically extracted centerline.

2.4 Results

Fig 2.2 shows an example of the extracted centerlines superimposed on the CTA image in 3D. No user interaction was needed and the approach was completely automated. The mean extraction error for this case was 2.55±0.70mm. In 1 training case and 2 testing cases, interaction was needed by the user to correct the centerline in the femoral artery. In the remaining 33 cases (91.7%), a fully automated centerline was obtained with excellent results.

Fig 2.3 shows the extraction error for each individual case. In all cases, the mean extraction error was 2.55±0.70mm (training 2.26±0.48mm versus testing 2.77±0.77mm, p = 0.03) and the average mean error was 1.63±0.40mm (training 1.46±0.35mm versus testing 1.74±0.39mm, p = 0.02).

The computational time for the algorithm to process each CTA dataset was 53±11 seconds, using a work station with Intel Core2 CPU (2.4 GHz) and 6 GB RAM.

2.5 Discussions

In this paper, we developed a completely automatic method to extract the arterial centerlines from whole-body CTA images. The validation results showed that 91.7% of the extracted arterial centerlines did not need any further user correction. The CTA images that were used in the validation were acquired by different systems in two clinical centers, demonstrating the robustness of the method.

Many papers have been published on coronary centerline extraction in CTA images, among which the method based on Hessian filter such as vesselness has been widely applied. Yang et al. (Yang et al. 2012) introduced a fully automatic method to extract coronary artery based on vesselness filter. This method cannot be directly applied to whole-body CTA scans, since the size of arteries in the entire access path generally demonstrates large inhomogeneity. Other methods such as morphological operation (Schaap et al. 2009) and histogram segmentation can lead to discontinuity in the centerline extraction when significant stenosis is present.

Our future work will focus on the automatic segmentation of lumen contour of the entire access route, the aortic valve, and the implementation of various quantitative parameters that could lead towards efficient and objective TAVR planning.

2.6 Conclusions

This method is robust and effective to extract arterial centerline automatically from whole-body CTA data sets. This is a first and important step towards efficient planning of TAVR procedures.

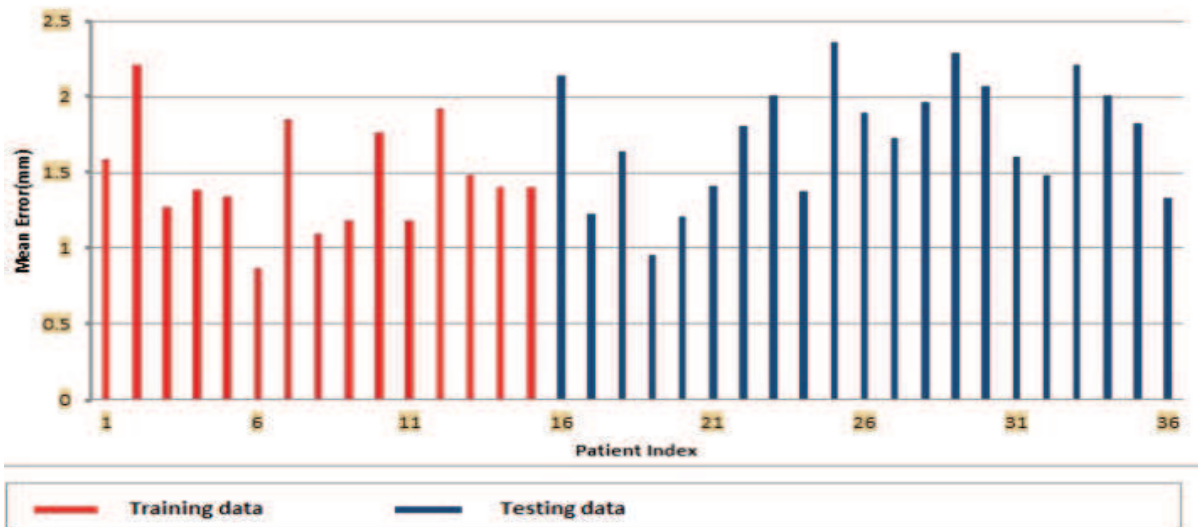**Fig 2.2.** Three-dimensional volume rendering and the extracted vascular centerline (yellow curve).

Figure 2.3. Distribution of mean extraction error.